

ACT-03-08, MIFP-08-19

# Yukawa Corrections from Four-Point Functions in Intersecting D6-Brane Models

Ching-Ming Chen,<sup>1</sup> Tianjun Li,<sup>1,2</sup> V. E. Mayes,<sup>1</sup> and D. V. Nanopoulos<sup>1,3</sup>

<sup>1</sup>*George P. and Cynthia W. Mitchell Institute for Fundamental Physics, Texas A&M University,  
College Station, TX 77843, USA*

<sup>2</sup>*Institute of Theoretical Physics, Chinese Academy of Sciences, Beijing 100080, China*

<sup>3</sup>*Astroparticle Physics Group, Houston Advanced Research Center (HARC),*

*Mitchell Campus, Woodlands, TX 77381, USA;*

*Academy of Athens, Division of Natural Sciences,*

*28 Panepistimiou Avenue, Athens 10679, Greece*

## Abstract

We discuss corrections to the Yukawa matrices of the Standard Model (SM) fermions in intersecting D-brane models due to four-point interactions. Recently, an intersecting D-brane model has been found where it is possible to obtain correct masses and mixings for all quarks as well as the tau lepton. However, the masses for the first two charged leptons come close to the right values but are not quite correct. Since the electron and muon are quite light, it is likely that there are additional corrections to their masses which cannot be neglected. With this in mind, we consider contributions to the SM fermion mass matrices from four-point interactions. In an explicit model, we show that it is indeed possible to obtain the SM fermion masses and mixings which are a better match to those resulting from experimental data extrapolated at the unification scale when these corrections are included. These corrections may have broader application to other models.

PACS numbers: 11.10.Kk, 11.25.Mj, 11.25.-w, 12.60.Jv

arXiv:0807.4216v2 [hep-th] 12 Sep 2008

## I. INTRODUCTION

In recent years, intersecting D-brane models, where the chiral fermions arise at the intersections between D6-branes (Type IIA) in the internal space [1] with the T-dual Type IIB description in terms of magnetized D-branes [2] have provided an exciting approach towards constructing semi-realistic string vacua (for reviews, see [3, 4]). Indeed, such models provide promising setups which may accommodate semi-realistic features of low-energy physics. Given this, it is an interesting question to see how far one can get from a particular string compactification to reproducing the finer details of the Standard Model (SM) as a low-energy effective field theory.

The Standard Model has an intricate structure, with three-generations of chiral fermions which transform as bifundamental representations of  $SU(3)_C \times SU(2)_L \times U(1)_Y$ . In addition to the fact that the SM fermions are replicated into three distinct generations, the different generations exhibit a distinct pattern of mass hierarchies and mixings. Interestingly, intersecting D-brane models may naturally generate the SM fermion mass hierarchies and mixings, as well as an explanation for the replication of chirality. In short, D6-branes (in Type IIA) fill four-dimensional Minkowski space-time and wrap 3-cycles in the compact manifold, with a stack of  $N$  D6-branes having a gauge group  $U(N)$  (or  $U(N/2)$  in the case of  $\mathbf{T}^6/(\mathbb{Z}_2 \times \mathbb{Z}_2)$ ) in its world volume. The 3-cycles wrapped by the D-branes will in general intersect multiple times in the internal space, resulting in chiral fermions in the bifundamental representation localized at the intersections between different stacks. The multiplicity of such fermions is then given by the number of times the 3-cycles intersect.

The Yukawa couplings in intersecting D6-brane models arise from open string world-sheet instantons that connect three D6-brane intersections [5]. For a given triplet of intersections, the minimal world-sheet action which contributes to the trilinear Yukawa couplings is weighted by a factor  $\exp(-A_{abc})$ , where  $A_{abc}$  is the world-sheet area of the triangle bounded by the branes  $a$ ,  $b$ , and  $c$ . Since there are several possible triangles with different areas, mass hierarchies may inherently arise. The Yukawa couplings depend on both the D-brane positions in the internal space as well as on the geometry of the underlying compact manifold. Effectively, these quantities are parameterized by the vacuum expectation values (VEVs) of open and closed-string moduli.

Despite substantial progress in constructing semi-realistic vacua with intersecting D-branes, there are many phenomenological challenges remaining, besides the usual moduli stabilization problem. Typically, some or all of the Yukawa couplings are typically forbidden by selection rules which arise from global  $U(1)$ s which become massive via a generalized Green-Schwarz mechanism. It has been found that only Pati-Salam models can have all the SM fermion Yukawa couplings

present at the stringy tree level, although some couplings which are perturbatively forbidden may be generated in principle via D-brane instanton effects [6, 7, 8, 9, 10]. Also, there has generally been a rank one problem in the SM fermion Yukawa matrices, preventing the generation of masses and mixings for the first two families of quarks and leptons. For the case of toroidal orientifold compactifications, this can be traced to the fact that not all of the SM fermions are localized at intersections on the same torus [11, 12, 13, 14]. However, one example of an intersecting D6-brane model in Type IIA on the  $\mathbf{T}^6/(\mathbb{Z}_2 \times \mathbb{Z}_2)$  orientifold has recently been discovered in which these problems may be solved [15, 16]. Thus, this particular model may be a step forward to obtaining realistic phenomenology from string theory. Indeed, as we have recently shown [17], it is possible within the moduli space of this model to obtain the correct SM quark masses and mixings, the tau lepton mass, and to generate naturally small neutrino masses via the seesaw mechanism. In addition to these features, the model exhibits automatic gauge coupling unification, and it is possible to generate realistic low-energy supersymmetric particle spectra, a subset of which may produce the observed dark matter density.

In spite of the successes of this model, the electron and muon masses come close to the right values, but they are still not quite correct. Since the electron and muon masses are very light, it is likely that there are additional corrections that must be considered, as first suggested a long time ago in [18]. This idea was applied later in string theory, for the case of the free-fermionic-formulation, where the general rules for calculating higher order corrections, from multipoint-functions, to the Yukawa couplings were first given in [19]. With this in mind, in this paper we consider contributions to the Yukawa couplings from four-point functions. Four-point string interactions in intersecting D6-brane scenarios can be regarded as the scattering amplitudes of four string matter fields [20], and are consistent to the Kähler metrics of twisted matter [21]. Both the quantum and classical contributions have been studied in two special cases where one has only an independent angle and the other has two independent angles in a closed quadrilateral [22]. This was then promoted to the generalized calculation of  $N$ -point amplitudes and four-point functions without angle constraints [23]. This analysis is based on the discussion of the twisted closed string interactions on orbifolds [24, 25, 26], where the analogy between open strings at brane intersections and closed strings on orbifolds is known. The complete amplitudes for Yukawa couplings, as a three-point limit of the four-point amplitude from conformal field theory, are also discussed in [20, 22, 23].

It is natural to ask whether the four-point function corrections to the Yukawa couplings can generate the correct electron and muon masses in the model discussed in [17]; indeed the correct

electron and muon masses can be obtained by including four-point function corrections in principle. However, the D6-branes in this model can not form a closed quadrilateral for the required four-point couplings on the relevant two torus. Two stacks of D-branes overlap so the “angle” at their “intersection” turns out as a straight line. Instead of using the conventional calculational procedure in this model, we can still apply the idea of four-point function corrections by taking the vector-like fields at the “intersection” on the overlapped D6-branes in a asymptotic limit of the “angle” to  $\pi$ , a physical mechanism which has not yet been clarified. Therefore, we shall consider another model where the standard four-point function corrections can be calculated. As we shall see later in this model, if the SM fermion mass matrices receive contributions from only three-point functions, one can only obtain the correct quark masses and tau lepton mass, but it is not possible to explain the CKM quark mixings, and the electron and muon masses. Introducing corrections from four-point functions, one can indeed obtain the correct quark and the tau lepton masses, and the CKM quark mixings, and as well as the electron mass. However, the muon mass is still about 36% smaller than the desired value.

In this paper, we review the construction of four-point functions, and include both trilinear Yukawa couplings and four-point interactions to obtain the SM fermion mass matrices in an explicit intersecting D-brane model. We show that it is indeed possible to better match the masses and mixings for all fermions when four-point corrections are included. In addition, these corrections may have broader application to other models.

## II. GENERAL FOUR-POINT FUNCTIONS

Let us begin by considering an open string stretched between two D-branes intersecting at an angle  $\pi\theta$ . From the boundary conditions we can write the mode expansion as

$$\begin{aligned}\partial X(z) &= \sum_k \alpha_{k-\theta} z^{-k+\theta-1}, \\ \partial \bar{X}(z) &= \sum_k \bar{\alpha}_{k-\theta} z^{-k-\theta-1},\end{aligned}\tag{1}$$

where  $z$  is the worldsheet coordinate. By comparison of this expression with the mode expansion for a closed string in the CFT analysis of a  $\mathbb{Z}_N$  orbifold twist field [24, 25, 26], the OPE can be written as [23]

$$\begin{aligned}\partial X(z)\sigma_\theta(w, \bar{w}) &\sim (z-w)^{-(1-\theta)}\tau_\theta(w, \bar{w}), \\ \partial \bar{X}(z)\sigma_\theta(w, \bar{w}) &\sim (z-w)^{-\theta}\tau'_\theta(w, \bar{w}),\end{aligned}\tag{2}$$

where  $X(w, \bar{w})$  is the intersection point of the two D-branes,  $\sigma_\theta(w, \bar{w})$  is the open string twist field, and  $\tau$  and  $\tau'$  are excited twist fields. The local monodromy conditions are then given by [23]

$$\begin{aligned}\partial X(e^{2\pi i}(z-w)) &= e^{2\pi i}\partial X(z-w), \\ \partial \bar{X}(e^{2\pi i}(z-w)) &= e^{-2\pi i}\partial \bar{X}(z-w).\end{aligned}\tag{3}$$

Since we are interested in a four-point interaction, we demand that the four strings are in a bounded area such that  $\sum \theta_i = 2$ , and it is required that the four twist operators  $\sigma_{\theta_i}(z_i, \bar{z}_i)$  are present at the D-brane intersections. Due to invariance under  $SL(2, \mathbb{R})$ , we can set  $z_1 = 0$ ,  $z_2 = x$ ,  $z_3 = 1$ , and  $z_4 = x_\infty$ . The field  $X$  has a classical piece  $X_{cl}$  and a quantum piece  $X_{qu}$ , so the interaction amplitude can be factorized into a classical solution resulting from worldsheet instantons and a quantum contribution resulting from quantum fluctuations as

$$Z = \sum_{\langle X_{cl} \rangle} e^{-S_{cl}} Z_{qu},\tag{4}$$

where

$$S_{cl} = \frac{1}{4\pi\alpha'} \int d^2z (\partial X_{cl} \bar{\partial} \bar{X}_{cl} + \bar{\partial} X_{cl} \partial \bar{X}_{cl}).\tag{5}$$

### A. The Classical Contribution

The classical field can be expanded by OPE as

$$\begin{aligned}\partial X_{cl}(z) &= a \omega(z), & \partial \bar{X}_{cl}(z) &= \bar{a} \omega'(z), \\ \bar{\partial} X_{cl}(\bar{z}) &= b \bar{\omega}'(\bar{z}), & \bar{\partial} \bar{X}_{cl}(\bar{z}) &= \bar{b} \bar{\omega}(\bar{z}),\end{aligned}\tag{6}$$

where

$$\omega(z) = \prod_i (z - x_i)^{-(1-\theta_i)}, \quad \omega'(z) = \prod_i (z - x_i)^{-\theta_i},\tag{7}$$

$a, \bar{a}, b$ , and  $\bar{b}$  are complex constants. On a torus with brane intersection considered [23], the local monodromy condition is given by

$$X(e^{2\pi i}z, e^{-2\pi i}\bar{z}) = e^{2\pi i\theta} X + (1 - e^{2\pi i\theta})(f + v),\tag{8}$$

where  $f$  is the intersection point and  $v$  is the lattice translation of the torus. Then from the global monodromy conditions we have [23]

$$\Delta_{C_i} X_{cl} = 4e^{-\pi i(\theta_i - \theta_{i+1})} \sin \pi \theta_i \sin \pi \theta_{i+1} (f_{i+1} - f_i + v_i) = \oint_{C_i} (dz \partial X_{cl}(z) + d\bar{z} \bar{\partial} X_{cl}(\bar{z})).\tag{9}$$

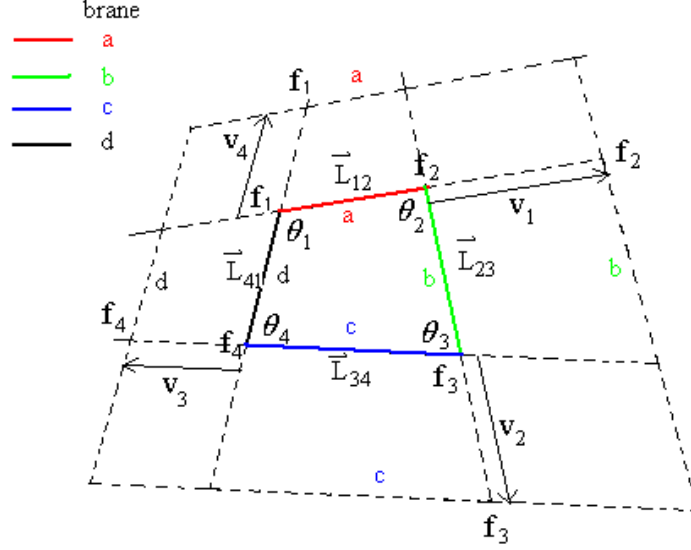


FIG. 1: Definition of the indices of the vertex and D-branes.

In Fig. 1, the index  $i$  denotes the  $i$ -th vertex,  $f_i$  is the intersection point between stack  $a$  and  $b$  D-branes and so on, and we define  $\vec{L}_{i,i+1}$  to be the vector along the direction from  $f_i$  to  $f_{i+1}$ . Thus  $v_1 = q_1 |I_{ab}| \vec{L}_{12}$ , etc, where  $q_i$  is an integer and  $I_{ab}$  is the intersection number. From the closure of the quadrilateral  $\sum v_i = 0$ , we can count the areas from the solutions of the linear diophantine equations [23]

$$\begin{pmatrix} q_1 I_{ba} \\ q_2 I_{ba} \end{pmatrix} = \begin{pmatrix} I_{cb} & I_{db} \\ I_{ac} & I_{ad} \end{pmatrix} \begin{pmatrix} q_3 \\ q_4 \end{pmatrix}. \quad (10)$$

In the case having two independent angles which we will consider later for a specific model, if stacks  $a$  and  $c$  are parallel to each other, then the above diophantine equations can be simplified, and the four integer parameters  $q_i$  are not independent. From [23] these  $q_i$  can be parameterized by two independent integer variables, which we will use in the following area analysis by applying a different approach.

Refer to [23] for the details of the calculation involving hypergeometric functions from the integral of  $\omega$  and  $\omega'$ , we can write down the minimum classical action when there is non-zero worldsheet area on one subtorus as [23]

$$S_{cl}^{T^2 \min} = \frac{1}{2\pi\alpha'} \left( \frac{\sin \pi\theta_1 \sin \pi\theta_4}{\sin(\pi\theta_1 + \pi\theta_4)} \frac{v_{14}^2}{2} + \frac{\sin \pi\theta_2 \sin \pi\theta_3}{\sin(\pi\theta_2 + \pi\theta_3)} \frac{v_{23}^2}{2} \right), \quad (11)$$

where the equation in the parenthesis is exactly the formula for the area of a quadrilateral with

angles  $\theta_i$  and two sides  $v_{14}$  and  $v_{23}$ . We will then use this information to calculate the classical contribution of the four-point functions.

## B. The Quantum Contribution

The quantum contribution of the four-point function is given by the correlator

$$\langle \sigma_{\theta_1}(z_1)\sigma_{\theta_2}(z_2)\sigma_{\theta_3}(z_3)\sigma_{\theta_4}(z_4) \rangle. \quad (12)$$

From the OPE of the stress tensor  $T(z)$  with the twist fields we have

$$T(z)\sigma_{\theta_j}(z_i) \sim \frac{h_j}{(z-z_i)^2} + \frac{\partial_{z_i}\sigma_{\theta_j}(z_i)}{(z-z_i)} + \dots, \quad (13)$$

where  $h_j = \frac{1}{2}\theta_j(1-\theta_j)$  is the conformal dimension.  $T(z)$  also has a relation to  $X$  as follows

$$-\frac{1}{2}\partial_z X \partial_w \bar{X} \sim \frac{1}{(z-w)^2} + T(z) + \dots. \quad (14)$$

Therefore, we can write

$$\begin{aligned} & \frac{\langle T(z)\sigma_{\theta_1}(z_1)\sigma_{\theta_2}(z_2)\sigma_{\theta_3}(z_3)\sigma_{\theta_4}(z_4) \rangle}{\langle \sigma_{\theta_1}(z_1)\sigma_{\theta_2}(z_2)\sigma_{\theta_3}(z_3)\sigma_{\theta_4}(z_4) \rangle} \\ &= \lim_{z \rightarrow w} \left[ \frac{\langle -\frac{1}{2}\partial_z X \partial_w \bar{X} \sigma_{\theta_1}(z_1)\sigma_{\theta_2}(z_2)\sigma_{\theta_3}(z_3)\sigma_{\theta_4}(z_4) \rangle}{\langle \sigma_{\theta_1}(z_1)\sigma_{\theta_2}(z_2)\sigma_{\theta_3}(z_3)\sigma_{\theta_4}(z_4) \rangle} - \frac{1}{(z-w)^2} \right]. \end{aligned} \quad (15)$$

We may then define the Green's function as

$$g(z, w; z_i) = \frac{\langle -\frac{1}{2}\partial_z X \partial_w \bar{X} \sigma_{\theta_1}(z_1)\sigma_{\theta_2}(z_2)\sigma_{\theta_3}(z_3)\sigma_{\theta_4}(z_4) \rangle}{\langle \sigma_{\theta_1}(z_1)\sigma_{\theta_2}(z_2)\sigma_{\theta_3}(z_3)\sigma_{\theta_4}(z_4) \rangle}. \quad (16)$$

From Eq. (14) we can find the asymptotic properties of  $g(z, w; z_i)$ :

$$\begin{aligned} g(z, w; z_i) &\sim \frac{1}{(z-w)^2} + \text{finite} && \text{for } z \rightarrow w, \\ &\sim \frac{1}{(z-z_i)^{-\theta_i}} && \text{for } z \rightarrow z_i, \\ &\sim \frac{1}{(w-z_i)^{-(1-\theta_i)}} && \text{for } w \rightarrow z_i. \end{aligned} \quad (17)$$

Similarly from Eqs. (1) and (7) we can write down the equations for  $X$  and  $\bar{X}$ :

$$\begin{aligned} \partial X(z) &\sim \omega_{\theta_i}(z) = \prod (z-x_i)^{-(1-\theta_i)}, \\ \partial \bar{X}(z) &\sim \omega'_{\theta_i}(z) = \prod (z-x_i)^{-\theta_i} = \omega_{1-\theta_i}(z). \end{aligned} \quad (18)$$

Then  $g(z, w; z_i)$  can be expanded in the following form [22, 23]

$$g(z, w; z_i) = \omega_{\theta_i}(z)\omega'_{\theta_i}(z) \left\{ \sum_{ij} a_{ij} \frac{(z-z_i)(z-z_j) \prod_k (w-z_k)}{(w-z_i)(w-z_j)(z-w)^2} + A \right\}. \quad (19)$$

The coefficients  $a_{ij}$  can be fixed by the above asymptotic relations, so finally we can determine

$$\begin{aligned} & \frac{\langle T(z)\sigma_{\theta_1}(z_1)\sigma_{\theta_2}(z_2)\sigma_{\theta_3}(z_3)\sigma_{\theta_4}(z_4) \rangle}{\langle \sigma_{\theta_1}(z_1)\sigma_{\theta_2}(z_2)\sigma_{\theta_3}(z_3)\sigma_{\theta_4}(z_4) \rangle} \\ &= -\frac{1}{2} \sum \theta_i \theta_j \frac{1}{(z-z_i)(z-z_j)} + \frac{1}{2} \sum_{i<j} a_{ij} \left( \frac{1}{z-z_i} + \frac{1}{z-z_j} \right)^2 + \frac{A}{\prod(z-z_i)}. \end{aligned} \quad (20)$$

The quantum part of the monodromy conditions is independent of the contours, so that

$$\Delta_{C_i} X_{qu} = 0 = \oint_{C_i} dz \partial X_{qu} + \oint_{C_i} d\bar{z} \bar{\partial} X_{qu}. \quad (21)$$

We can use this condition to determine  $A$  and define two homology cycles  $C_1$  and  $C_2$  by cutting the complex plane between  $z_1$  and  $z_2$ , and between  $z_3$  and  $z_4$ . In this way, we find

$$\oint_{C_i} dz g(z, w) + \oint_{C_i} d\bar{z} h(\bar{z}, w) = 0, \quad (22)$$

where  $h(\bar{z}, w)$  is the auxiliary correlation function

$$h(\bar{z}, w; z_i) \equiv \frac{\langle -\frac{1}{2} \partial_{\bar{z}} X \partial_w \bar{X} \sigma_{\theta_1}(z_1) \sigma_{\theta_2}(z_2) \sigma_{\theta_3}(z_3) \sigma_{\theta_4}(z_4) \rangle}{\langle \sigma_{\theta_1}(z_1) \sigma_{\theta_2}(z_2) \sigma_{\theta_3}(z_3) \sigma_{\theta_4}(z_4) \rangle} = B \bar{\omega}_{1-\theta_i}(\bar{z}) \omega'_{\theta_i}(z). \quad (23)$$

After using the  $SL(2, \mathbb{R})$  invariance, we obtain that Eq. (21) turns out to be

$$B \oint_{C_i} \bar{\omega}'(\bar{z}) d\bar{z} + A \oint_{C_i} \omega(z) dz = x_{\infty} \oint_{C_i} \sum_i a_{i4} (z - x_i) \omega(z) dz. \quad (24)$$

Solving  $A$ , the correlator  $\langle \sigma_{\theta_1} \sigma_{\theta_2} \sigma_{\theta_3} \sigma_{\theta_4} \rangle$  then has a form [23]

$$\langle \sigma_{\theta_1} \sigma_{\theta_2} \sigma_{\theta_3} \sigma_{\theta_4} \rangle = |I(x)|^{-\frac{1}{2}} x_{\infty}^{-\theta_4(1-\theta_4)} x^{\frac{1}{2}(\theta_1+\theta_2-1)-\theta_1\theta_2} (1-x)^{\frac{1}{2}(\theta_2+\theta_3-1)-\theta_2\theta_3}, \quad (25)$$

where  $I(x)$  is a function of  $x$ ,  $\theta_i$ , gamma functions of  $\theta_i$ , and hypergeometric functions [23].

Again, we are more interested in the case with two independent angles, therefore by setting  $\theta_1 = 1 - \theta_2 = \nu$  and  $\theta_4 = 1 - \theta_3 = \lambda$ , the quantum part of the four-point function can be written as [22, 23]

$$Z_{4q} = 16\pi^{\frac{5}{2}} x^{-\nu(1-\nu)} (1-x)^{-\nu\lambda} I(x)^{-\frac{1}{2}}, \quad (26)$$

where

$$\begin{aligned} I(x) &= (1-x)^{(1-\nu-\lambda)} \left[ B(\nu, \lambda) {}_2F_1(\nu, \lambda, \nu + \lambda; 1-x) {}_2F_1(1-\nu, 1-\lambda, 1; x) \right. \\ &\quad \left. + B(1-\nu, 1-\lambda) {}_2F_1(1-\nu, 1-\lambda, 2-\nu-\lambda; 1-x) {}_2F_1(\nu, \lambda, 1; x) \right], \end{aligned} \quad (27)$$

and  ${}_2F_1$  is the hypergeometric function;  $B(\nu, \lambda) = \Gamma(\nu)\Gamma(\lambda)/\Gamma(\nu + \lambda)$ . We have used the fact that  ${}_2F_1(\nu, \lambda, 1; x) = (1-x)^{(1-\nu-\lambda)} {}_2F_1(1-\nu, 1-\lambda, 1; x)$ . Note that the quantum contribution Eq. (26) remains invariant under the interchange of the interior and exterior angles  $\nu, \lambda \leftrightarrow 1-\nu, 1-\lambda$ .



The general form for a four-point amplitude on  $\mathbf{T}^6$  with two independent angles is then given by

$$Z_4 = 16\pi^{5/2} \prod_j x_j^{-\nu_j(1-\nu_j)} (1-x_j)^{-\nu_j\lambda_j} I_j(x_j)^{-1/2} \sum_{k,l} \exp\left(-\frac{A_{4j}}{2\pi\alpha'}\right). \quad (28)$$

By taking the limit of  $x$ ,  $Z_{3q}$  is fixed to a constant and we obtain the three-point amplitude for the Yukawa couplings [20, 22]

$$Z_3 = 2\pi \prod_j \left[ \frac{16\pi^2 \Gamma(1-\nu_j) \Gamma(1-\lambda_j) \Gamma(\nu_j + \lambda_j)}{\Gamma(\nu_j) \Gamma(\lambda_j) \Gamma(1-\nu_j - \lambda_j)} \right]^{1/4} \sum_m \exp\left(-\frac{A_j}{2\pi\alpha'}\right). \quad (29)$$

As we will later encounter in the model considered in the next section, where only the D-branes on the second torus form closed areas either for four-point or three-point amplitudes, the quantum contributions from other tori are just constants, which are then able to be absorbed into the VEVs of the Higgs fields. Using a computer code, we find that the ratio of  $Z_{4q}$  to  $Z_{3q}$  is around  $\mathcal{O}(10)$  which can then also be absorbed into the VEVs for simplicity. Therefore, we can merely focus on the classical contributions to the SM fermion masses and mixings.

### III. A WORKING EXAMPLE OF THE SM FERMION MASSES AND MIXINGS

#### A. The Pati-Salam Models

Let us first review the Pati-Salam model discussed in [17], where its D6-brane configurations and intersecting numbers are presented in Table I. To explain the electron and muon masses in this model, we are looking for four-point interactions such as

$$\phi_{ab}^i \phi_{ca}^j \phi_{b'c}^k \phi_{bb'}^l \quad \text{or} \quad \phi_{ab}^i \phi_{ca}^j \phi_{cc'}^k \phi_{bc'}^l, \quad (30)$$

where  $\phi_{\alpha\beta}^i$  are the chiral superfields at the intersections between stack  $\alpha$  and  $\beta$  D6-branes.

stk	$N$	$(n_1, l_1)$	$(n_2, l_2)$	$(n_3, l_3)$
$a$	8	( 0,-1)	( 1, 1)	( 1, 1)
$b$	4	( 3, 1)	( 1, 0)	( 1,-1)
$c$	4	( 3,-1)	( 0, 1)	( 1,-1)

TABLE I: D6-brane configurations and intersecting numbers for the model presented in [17], where the SM fermions and Higgs fields are from the intersections on the first torus. This model is constructed from Type IIA  $\mathbf{T}^6/(\mathbb{Z}_2 \times \mathbb{Z}_2)$  orientifold.

From Table I, considering the wrapping numbers on the first two-torus, we find that the  $\Omega R$  image  $b'$  of stack  $b$  is parallel to stack  $c$ , and stack  $b$  is parallel to the  $\Omega R$  image  $c'$  of stack  $c$ . It is

required that  $b$  and  $c'$  or  $c$  and  $b'$  must overlap to form a closed area, which is not exactly forming a quadrilateral. After carefully studying the possible four-point functions on the first torus, we find that we can obtain the correct electron and muon masses. However, the techniques for calculating such kind of geometric structure for four-point functions have not been clarified yet. Therefore, we turn our attention to the other models. To avoid the generic rank one problem, we require that the three SM fermion families arise from the intersections on the same two-torus. The number of the Higgs bidoublets from that torus is a multiple of 3. In addition, we require that the  $\Omega R$  image of the  $U(2)_L$  D-brane stack forms a closed quadrilateral with the  $U(4)$ ,  $U(2)_L$ , and  $U(2)_R$  stacks to get rid of exotic particles. And there may also arise additional constraints on the D-brane wrapping numbers to form a bounded area. Generally a three-generation model without exotic SM type particles has a structure like that of a stack of D-branes which lies on the orbifold while the other two are images of each other and the ratio of the wrapping numbers is three, for example  $(n, m) = (1, 3)$ , just as the model discussed in [17]. However, similar to the above model, we find that such types of models cannot form a normal bounded four-point area. Thus, we will consider the Model TI-U-3 in [16]. We present its D6-brane configurations and intersecting numbers of the observable sector in Table II, and the particle spectrum of the observable sector in Table III, where  $S_L^i$  and  $\bar{S}_L^i$  are the SM singlets from the intersections of stack  $b$  and its  $\Omega R$  image  $b'$ .

stk	$N$	$(n_1, l_1)(n_2, l_2)(n_3, l_3)$	A	S	$b$	$b'$	$c$	$c'$	$d$	$O6$
$a$	4	( 1, 1) ( 1,-3) ( 1, 0)	0	0	3	0(1)	-3	0(3)	-3	0(3)
$b$	2	( 2, 0) ( 1, 3) ( 1,-1)	0	0	-	-	6	0(3)	6	0(3)
$c$	2	( 1,-1) ( 2, 0) ( 1, 1)	0	0	-	-	-	-	0(1)	0(1)

TABLE II: D6-brane configurations and intersecting numbers in the Model TI-U-3 in [16], where the SM fermions and three of the six Higgs fields are from the intersections on the second two-torus. This model is constructed in the supersymmetric AdS vacuum on Type IIA  $\mathbf{T}^6$  orientifold with flux compactifications.

The superpotential which includes the trilinear Yukawa couplings is given by

$$\mathcal{W}_3 \sim Y_{ijk}^u Q^i U^{cj} H_u^k + Y_{ijk}^d Q^i D^{cj} H_d^k + Y_{ijk}^l L^i E^{cj} H_d^k, \quad (31)$$

where  $Y_{ijk}^u$ ,  $Y_{ijk}^d$ , and  $Y_{ijk}^l$  are Yukawa couplings, and  $Q^i$ ,  $U^{ci}$ ,  $D^{ci}$ ,  $L^i$  and  $E^{ci}$  are the left-handed quark doublet, right-handed up-type quarks, right-handed down-type quarks, left-handed lepton doublet, and right-handed leptons, respectively. The superpotential including the four-point interactions is

$$\mathcal{W}_4 \sim \frac{1}{M_S} \left( Y_{ijkl}^{tu} Q^i U^{cj} H_u^k S_L^l + Y_{ijkl}^{td} Q^i D^{cj} H_d^k S_L^l + Y_{ijkl}^{tl} L^i E^{cj} H_d^k S_L^l \right), \quad (32)$$

	Quantum Number	$Q_4$	$Q_{2L}$	$Q_{2R}$	Field
$ab$	$3 \times (4, \bar{2}, 1, 1)$	1	-1	0	$F_L(Q_L, L_L)$
$ac$	$3 \times (\bar{4}, 1, 2, 1)$	-1	0	1	$F_R(Q_R, L_R)$
$ac'$	$3 \times (4, 1, 2, 1)$	1	0	1	$\Phi_i$
	$3 \times (\bar{4}, 1, \bar{2}, 1)$	-1	0	-1	$\bar{\Phi}_i$
$bc$	$6 \times (1, 2, \bar{2}, 1)$	0	1	-1	$H_u^i, H_d^i$
	$6 \times (1, \bar{2}, 2, 1)$	0	-1	1	
$b'c$	$3 \times (1, \bar{2}, \bar{2}, 1)$	0	-1	-1	$H'_u, H'_d$
	$3 \times (1, 2, 2, 1)$	0	1	1	
$b'b$	$6 \times (1, 1, 1, 1)$	0	2	0	$S_L^i$
	$6 \times (1, \bar{1}, 1, 1)$	0	-2	0	$\bar{S}_L^i$

TABLE III: The chiral and vector-like superfields in the observable sector, and their quantum numbers under the gauge symmetry  $SU(4)_C \times SU(2)_L \times SU(2)_R$ .

where  $Y_{ijkl}^{tu}$ ,  $Y_{ijkl}^{td}$ , and  $Y_{ijkl}^l$  are Yukawa couplings of the four-point functions, and  $M_G$  is the string scale.

### B. Yukawa Couplings from Three-Point Functions

In order to calculate the trilinear Yukawa couplings, we first note the intersection numbers on three two-tori

$$\begin{aligned}
I_{ab}^{(1)} &= -1, & I_{ab}^{(2)} &= 3, & I_{ab}^{(3)} &= -1, \\
I_{ca}^{(1)} &= 1, & I_{ca}^{(2)} &= -3, & I_{ca}^{(3)} &= -1, \\
I_{bc}^{(1)} &= -1, & I_{bc}^{(2)} &= -3, & I_{bc}^{(3)} &= 2.
\end{aligned} \tag{33}$$

From these, we find that  $d^{(2)} = g.c.d.(I_{ab}^{(2)}, I_{bc}^{(2)}, I_{ca}^{(2)}) = 3$ ,  $d^{(1)} = 1$ , and  $d^{(3)} = 1$ . The parameters of the theta functions in terms of the intersection numbers, the brane shifts  $\epsilon_\alpha^{(i)}$ , the Wilson line phases  $\theta_\alpha^{(i)}$ , and the Kähler moduli  $J^{(i)}$  are [11]

$$\begin{aligned}
\delta^{(1)} &= -\epsilon_c^{(1)} + \epsilon_b^{(1)} - \epsilon_a^{(1)}, \\
\delta^{(2)} &= \frac{i^{(2)}}{3} - \frac{j^{(2)}}{3} - \frac{k^{(2)}}{3} + \frac{\epsilon_c^{(2)} - \epsilon_b^{(2)} - \epsilon_a^{(2)}}{3} + \frac{s^{(2)}}{3}, \\
\delta^{(3)} &= \frac{k^{(3)}}{2} + \frac{-\epsilon_c^{(3)} - \epsilon_b^{(3)} + 2\epsilon_a^{(3)}}{2} + \frac{s^{(3)}}{2},
\end{aligned} \tag{34}$$

$$\begin{aligned}
\phi^{(1)} &= -\theta_c^{(1)} + \theta_b^{(1)} - \theta_a^{(1)}, \\
\phi^{(2)} &= \theta_c^{(2)} - \theta_b^{(2)} - \theta_a^{(2)}, \\
\phi^{(3)} &= -\theta_c^{(3)} - \theta_b^{(3)} + 2\theta_a^{(2)},
\end{aligned} \tag{35}$$

$$\kappa^{(1)} = \frac{J^{(1)}}{\alpha'}, \quad \kappa^{(2)} = \frac{3J^{(3)}}{\alpha'}, \quad \kappa^{(3)} = \frac{2J^{(3)}}{\alpha'}. \tag{36}$$

For convenience we redefine the shift on each torus as

$$\epsilon^{(1)} \equiv -\epsilon_c^{(1)} + \epsilon_b^{(1)} - \epsilon_a^{(1)}, \quad \epsilon^{(2)} \equiv \frac{\epsilon_c^{(2)} - \epsilon_b^{(2)} - \epsilon_a^{(2)}}{3}, \quad \epsilon^{(3)} \equiv \frac{-\epsilon_c^{(3)} - \epsilon_b^{(3)} + 2\epsilon_a^{(3)}}{2}, \tag{37}$$

then the theta function of each torus can be written as [11]

$$\vartheta \begin{bmatrix} \delta^{(r)} \\ \phi^{(r)} \end{bmatrix} (\kappa^{(r)}) = \sum_{l_r \in \mathbf{Z}} e^{\pi i (\delta^{(r)} + l_r)^2 \kappa^{(r)}} e^{2\pi i (\delta^{(r)} + l_r) \phi^{(r)}}, \tag{38}$$

where  $r = 1, 2, 3$ , so the Yukawa coupling constant can be expressed as

$$Y_{\{ijk\}} = Z_{3q} \sigma_{abc} \prod_{r=1}^3 \vartheta \begin{bmatrix} \delta^{(r)} \\ \phi^{(r)} \end{bmatrix} (\kappa^{(r)}), \tag{39}$$

where  $Z_{3q}$  stands for the quantum contribution to the instanton amplitude, and  $\sigma_{abc} = \prod_r \text{sign}(I_{ab}^{(r)} I_{bc}^{(r)} I_{ca}^{(r)})$ .

For the first torus the intersection number is one, so its contribution is just a constant. On the second torus  $i^{(2)}, j^{(2)}, k^{(2)}$  range from 0 – 2, and on the third torus  $k^{(3)}$  goes from 0 to 1. Thus, although the total number of Higgs state is  $k^{(2)} \times k^{(3)} = 3 \times 2 = 6$ , only three linear combinations of six Higgs fields can provide the SM fermion Yukawa couplings since the intersection number between  $b$  and  $c$  stacks of D6-brane is 3 on the second two-torus. Explicitly, there is only one SM Higgs linear combination from the two bidoublet fields  $(k^{(2)}, k^{(3)}) = \{(k^{(2)}, 0), (k^{(2)}, 1)\}$ . Furthermore, since the triplet of intersections is connected by an instanton, the selection rule for the indices of the second torus

$$i^{(2)} + j^{(2)} + k^{(2)} = 0 \pmod{3}, \tag{40}$$

should be satisfied. Then we can choose the Yukawa coupling matrices as the following form

$$Y_{k=0}^{(2)} \sim \begin{pmatrix} A & 0 & 0 \\ 0 & 0 & C \\ 0 & B & 0 \end{pmatrix}, \quad Y_{k=1}^{(2)} \sim \begin{pmatrix} 0 & 0 & B \\ 0 & A & 0 \\ C & 0 & 0 \end{pmatrix}, \quad Y_{k=2}^{(2)} \sim \begin{pmatrix} 0 & C & 0 \\ B & 0 & 0 \\ 0 & 0 & A \end{pmatrix}, \tag{41}$$

where

$$A \equiv \vartheta \begin{bmatrix} \epsilon^{(2)} \\ \phi^{(2)} \end{bmatrix} \left( \frac{3J^{(2)}}{\alpha'} \right), \quad B \equiv \vartheta \begin{bmatrix} \epsilon^{(2)} + \frac{1}{3} \\ \phi^{(2)} \end{bmatrix} \left( \frac{3J^{(2)}}{\alpha'} \right), \quad C \equiv \vartheta \begin{bmatrix} \epsilon^{(2)} - \frac{1}{3} \\ \phi^{(2)} \end{bmatrix} \left( \frac{3J^{(2)}}{\alpha'} \right), \quad (42)$$

where we simply set here  $s^{(2)} = k^{(2)}$ . Similarly in the third torus, there is only one parameter

$$Y_{k=0}^{(3)} \sim \vartheta \begin{bmatrix} \epsilon^{(3)} \\ \phi^{(3)} \end{bmatrix} \left( \frac{2J^{(3)}}{\alpha'} \right) \equiv A_3, \quad Y_{k=1}^{(3)} \sim \vartheta \begin{bmatrix} \epsilon^{(3)} + \frac{1}{2} \\ \phi^{(3)} \end{bmatrix} \left( \frac{2J^{(3)}}{\alpha'} \right) \equiv D_3. \quad (43)$$

Therefore the classical part of this three-point couplings is given by

$$\begin{aligned} Z_{3cl1} &= \begin{pmatrix} AA_3 & 0 & 0 \\ 0 & 0 & CA_3 \\ 0 & BA_3 & 0 \end{pmatrix}, \quad Z_{3cl2} = \begin{pmatrix} 0 & 0 & BA_3 \\ 0 & AA_3 & 0 \\ CA_3 & 0 & 0 \end{pmatrix}, \quad Z_{3cl3} = \begin{pmatrix} 0 & CA_3 & 0 \\ BA_3 & 0 & 0 \\ 0 & 0 & AA_3 \end{pmatrix}, \\ Z_{3cl4} &= \begin{pmatrix} AD_3 & 0 & 0 \\ 0 & 0 & CD_3 \\ 0 & BD_3 & 0 \end{pmatrix}, \quad Z_{3cl5} = \begin{pmatrix} 0 & 0 & BD_3 \\ 0 & AD_3 & 0 \\ CD_3 & 0 & 0 \end{pmatrix}, \quad Z_{3cl6} = \begin{pmatrix} 0 & CD_3 & 0 \\ BD_3 & 0 & 0 \\ 0 & 0 & AD_3 \end{pmatrix} \end{aligned} \quad (44)$$

If each of the Higgs states resulting from intersections localized between stacks  $b$  and  $c$  develops a VEV,  $v_i^\Phi$ , where  $i = 1, \dots, 6$  for each of the six Higgs states, and  $\Phi$  is an index for ( $u$ )p-type quarks, ( $d$ )own-type quarks, and ( $l$ )eptons, respectively, the total effects of Yukawa couplings including the quantum part will be

$$Z_3^\Phi = Z_{3q} \begin{pmatrix} A(A_3 v_1^\Phi + D_3 v_4^\Phi) & C(A_3 v_3^\Phi + D_3 v_6^\Phi) & B(A_3 v_2^\Phi + D_3 v_5^\Phi) \\ B(A_3 v_3^\Phi + D_3 v_6^\Phi) & A(A_3 v_2^\Phi + D_3 v_5^\Phi) & C(A_3 v_1^\Phi + D_3 v_4^\Phi) \\ C(A_3 v_2^\Phi + D_3 v_5^\Phi) & B(A_3 v_1^\Phi + D_3 v_4^\Phi) & A(A_3 v_3^\Phi + D_3 v_6^\Phi) \end{pmatrix}, \quad (45)$$

where  $v_i^{(d)} = v_i^{(l)}$ . Thus, it is clear that only three linear combinations of the six Higgs states contribute to the Yukawa couplings:  $A_3 H_1^\Phi + D_3 H_4^\Phi$ ,  $A_3 H_3^\Phi + D_3 H_6^\Phi$ , and  $A_3 H_2^\Phi + D_3 H_5^\Phi$ , where for simplicity we neglect the normalization.

### C. Yukawa Couplings from Four-Point Functions

The formula for the area of a quadrilateral in terms of its angles and two sides and the solutions of diophantine equations for estimating the multiple areas of the quadrilaterals from non-unit intersection numbers are given in [23]. In the present discussion, we are considering a model which possesses only two independent angles, so we need at least two parameters to describe all quadrilaterals. In addition to these formulae, there is a more intuitive way to calculate the area for

these four-sided polygons with only two independent angles. A quadrilateral with two independent angles is a trapezoid, and a trapezoid can be always taken as the difference between two similar triangles. Therefore, since we know the classical part is

$$Z_{4cl} \sim e^{-A_{quad}}, \quad (46)$$

it is equivalent to write

$$Z_{4cl} \sim e^{-|A_{tri} - A'_{tri}|}. \quad (47)$$

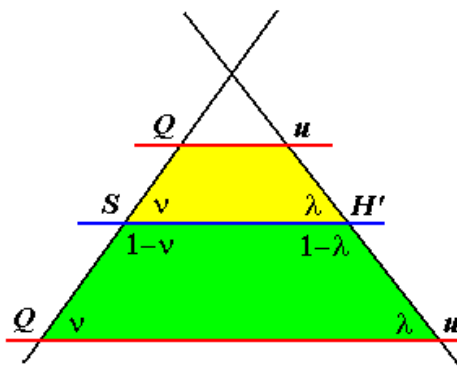


FIG. 2: A picture of two trapezoids with different field orders. The red brane repeats in a next cycle and can still form a similar trapezoid with the blue brane. This coupling also contributes to the four-point function.

Taking the absolute value of the difference reveals that there are two cases:  $A_{tri} > A'_{tri}$  and  $A_{tri} < A'_{tri}$ , as shown in Fig. 2. From the figure we can see the two trapezoids are similar with different sizes, but the orders of the fields corresponding to the angles are different, which is under an interchange of  $\theta \leftrightarrow 1 - \theta$ ,  $\theta = \nu, \lambda$ . These different field orders may cause different values for their quantum contributions. However, we have shown above that this angle transformation will not affect the quantum contribution, so these two cases are on equal foot to sum up. Therefore, we are able to employ the same techniques which have developed for calculating the trilinear Yukawa couplings.

For a trapezoid formed by the stacks  $a, b, b', c$ , we can calculate it as the difference between two triangles formed by stacks  $a, b, c$  and  $b', b, c$ . In other words, they share the same intersection  $I_{bc}$ . Therefore, if we use this method to calculate the trapezoidal area, we should keep in mind that the intersection index  $k$  for  $I_{bc}$  remains the same for a certain class of trapezoids when varying

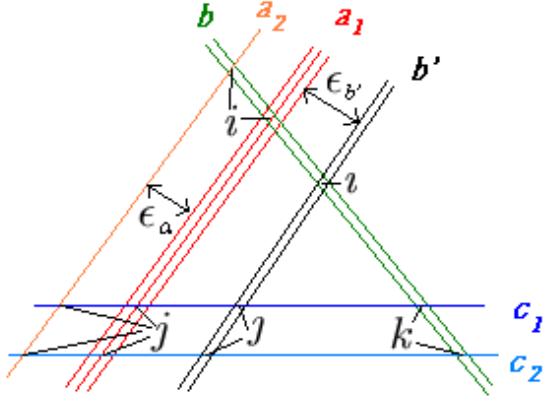


FIG. 3: A diagram showing the areas bounded by stacks of D-branes which give rise to the Yukawa couplings for quarks and leptons via world-sheet instantons. The Yukawa couplings of the up-type quarks are from the areas by stack  $a_1$ ,  $b$ ,  $c_1$ , the down-type quarks by stack  $a_1$ ,  $b$ ,  $c_2$ , and the leptons by  $a_2$ ,  $b$ ,  $c_2$ . The four-point function corrections to the Yukawa couplings of the up-type quarks are from the areas by stack  $a_1$ ,  $b$ ,  $b'$ ,  $c_1$ , the down-type quarks by stack  $a_1$ ,  $b$ ,  $b'$ ,  $c_2$ , and the leptons by  $a_2$ ,  $b$ ,  $b'$ ,  $c_2$ .

other intersecting indices. Here we set indices  $i$  for  $I_{ab}$ ,  $j$  for  $I_{ca}$ ,  $l$  for  $I_{b'b}$ , and  $j$  for  $I_{cb'}$ , as shown in Fig. 3. We may calculate the areas of the triangles as we did in the trilinear Yukawa couplings above [11]

$$\begin{aligned}
 A_{ijk} &= \frac{1}{2}(2\pi)^2 A_{\mathbf{T}^2} |I_{ab} I_{bc} I_{ca}| \left( \frac{i}{I_{ab}} + \frac{j}{I_{ca}} + \frac{k}{I_{bc}} + \epsilon + l \right)^2, \\
 A_{ljk} &= \frac{1}{2}(2\pi)^2 A_{\mathbf{T}^2} |I_{b'b} I_{bc} I_{cb'}| \left( \frac{l}{I_{b'b}} + \frac{j}{I_{cb'}} + \frac{k}{I_{bc}} + \epsilon + l \right)^2,
 \end{aligned} \tag{48}$$

where  $i$ ,  $j$ ,  $k$  and  $l$ ,  $j$ ,  $k$  are using the same selection rules as Eq. (40). Thus, the classical contribution of the four-point functions is given by

$$Z_{4cl} = \sum_{l,\ell} e^{-\frac{1}{2\pi} |A_{ijk} - A_{ljk}|}. \tag{49}$$

Note that this formula will diverge when  $A_{ijk} = A_{ljk}$ , which is due to over-counting the zero area when the corresponding parameters in Eq. (48) are the same. In such a case,  $Z_{4cl} = 1 + \sum_{l \neq \ell} e^{-\frac{1}{2\pi} |A_{ijk} - A_{ljk}|}$ . We will not meet this special situation in our following discussion.

In the model of Table II, in addition to the intersection numbers in Eq. (33), we have

$$\begin{aligned}
 I_{bb'}^{(1)} &= 0, & I_{bb'}^{(2)} &= -3, & I_{bb'}^{(3)} &= 2; \\
 I_{bO6}^{(1)} &= 0, & I_{bO6}^{(2)} &= -3, & I_{bO6}^{(3)} &= 2; \\
 I_{cb'}^{(1)} &= 1, & I_{cb'}^{(2)} &= -3, & I_{cb'}^{(3)} &= 0,
 \end{aligned} \tag{50}$$

and the number of the singlets from the  $SU(2)_L$  anti-symmetric representation is given by  $\mathcal{M}_{Anti} = \prod_i (I_{bb'}^{(i)} + I_{bO6}^{(i)})/2$ . It is obvious that we have six vector-like anti-symmetric fields for  $SU(2)_L$ , three from the second torus and two from the third torus. The matrix elements on the second torus from the four-point functions can be written in terms of  $a_{ij\ell j}$  as

$$\begin{aligned} & \begin{pmatrix} a_{0000} & 0 & 0 \\ 0 & 0 & a_{1200} \\ 0 & a_{2100} & 0 \end{pmatrix}, \begin{pmatrix} 0 & a_{0101} & 0 \\ a_{1001} & 0 & 0 \\ 0 & 0 & a_{2201} \end{pmatrix}, \begin{pmatrix} 0 & 0 & a_{0202} \\ 0 & a_{1102} & 0 \\ a_{2002} & 0 & 0 \end{pmatrix}, \\ & \begin{pmatrix} 0 & a_{0110} & 0 \\ a_{1010} & 0 & 0 \\ 0 & 0 & a_{2210} \end{pmatrix}, \begin{pmatrix} 0 & 0 & a_{0211} \\ 0 & a_{1111} & 0 \\ a_{2011} & 0 & 0 \end{pmatrix}, \begin{pmatrix} a_{0012} & 0 & 0 \\ 0 & 0 & a_{1212} \\ 0 & a_{2112} & 0 \end{pmatrix}, \\ & \begin{pmatrix} 0 & 0 & a_{0220} \\ 0 & a_{1120} & 0 \\ a_{2020} & 0 & 0 \end{pmatrix}, \begin{pmatrix} a_{0021} & 0 & 0 \\ 0 & 0 & a_{1221} \\ 0 & a_{2121} & 0 \end{pmatrix}, \begin{pmatrix} 0 & a_{0122} & 0 \\ a_{1022} & 0 & 0 \\ 0 & 0 & a_{2222} \end{pmatrix}. \end{aligned} \quad (51)$$

The relations between these elements are shown in Table IV.

Parameters	$\delta$	$d$	$k=0$	$k=1$	$k=2$
$\mathcal{A}$	0	0	$a_{0000}$	$a_{1111}$	$a_{2222}$
$\mathcal{B}$	$\frac{1}{3}$	0	$a_{2100}$	$a_{0211}$	$a_{1022}$
$\mathcal{C}$	$\frac{-1}{3}$	0	$a_{1200}$	$a_{2011}$	$a_{0122}$
$\mathcal{D}$	0	$\frac{1}{3}$	$a_{0021}$	$a_{1102}$	$a_{2210}$
$\mathcal{E}$	$\frac{1}{3}$	$\frac{1}{3}$	$a_{2121}$	$a_{0202}$	$a_{1010}$
$\mathcal{F}$	$\frac{-1}{3}$	$\frac{1}{3}$	$a_{1221}$	$a_{2002}$	$a_{0110}$
$\mathcal{G}$	0	$\frac{-1}{3}$	$a_{0012}$	$a_{1120}$	$a_{2201}$
$\mathcal{H}$	$\frac{1}{3}$	$\frac{-1}{3}$	$a_{2112}$	$a_{0220}$	$a_{1001}$
$\mathcal{I}$	$\frac{-1}{3}$	$\frac{-1}{3}$	$a_{1212}$	$a_{2020}$	$a_{0101}$

TABLE IV: The matrix elements in terms of parameters.  $\delta = \frac{i}{I_{ab}} + \frac{j}{I_{ca}} + \frac{k}{I_{bc}}$  and  $d = \frac{i}{I_{b'b}} + \frac{j}{I_{cb'}} + \frac{k}{I_{bc}}$ . Note that since we need to sum over  $l$  and  $\ell$ , an integer shift has no effect, so  $\frac{1}{3}$  is equivalent to  $\frac{-2}{3}$ ;  $\frac{-1}{3}$  is equivalent to  $\frac{2}{3}$  for  $d$  and  $\delta$ , etc.

In this model, we have six SM singlet fields  $S_L^i$  and three Higgs-like states  $H_{u,d}^i$ . Similar to the Higgs fields  $H_{u,d}^i$ , only three linear combinations of the six  $S_L^i$  can contribute to the four-point Yukawa couplings. Thus, the four-point Yukawa couplings involve three SM singlet fields  $S_L^i$  and three Higgs-like states  $H_{u,d}^i$ . If their VEVs are denoted as  $u_i$  and  $w_j$  respectively, then the complete



contribution will be

$$Z_{4cl} \sim \begin{pmatrix} \mathcal{A}u_1w_1 + \mathcal{G}u_2w_3 + \mathcal{D}u_3w_2 & \mathcal{I}u_1w_2 + \mathcal{F}u_2w_1 + \mathcal{C}u_3w_3 & \mathcal{E}u_1w_3 + \mathcal{B}u_2w_2 + \mathcal{H}u_3w_1 \\ \mathcal{H}u_1w_2 + \mathcal{E}u_2w_1 + \mathcal{B}u_3w_3 & \mathcal{D}u_1w_3 + \mathcal{A}u_2w_2 + \mathcal{G}u_3w_1 & \mathcal{C}u_1w_1 + \mathcal{I}u_2w_3 + \mathcal{F}u_3w_2 \\ \mathcal{F}u_1w_3 + \mathcal{C}u_2w_2 + \mathcal{I}u_3w_1 & \mathcal{B}u_1w_1 + \mathcal{H}u_2w_3 + \mathcal{E}u_3w_2 & \mathcal{G}u_1w_2 + \mathcal{D}u_2w_1 + \mathcal{A}u_3w_3 \end{pmatrix}. \quad (52)$$

#### IV. A NUMERICAL EXAMPLE

##### A. The SM Fermion Masses and Mixings at the GUT Scale

The main reason for the addition of these four-point corrections is to better match the Yukawa coupling matrices to those obtained by running the renormalization group equations (RGEs) up to the GUT scale. In particular, we would like to better match the lepton masses. It should be remembered that the parameters from the theta function and the parameters in Table IV which depend on the D-brane shift parameters are not independent. Thus, the different elements of the Yukawa mass matrix are related, as discussed in [17] which strongly constrains the form that they may take. As before, we will perform a transformation on the SM fermion mass matrices which are obtained from the RGE running of the experimental values for the SM fermion masses up to the GUT scale to make the comparison with the theoretical results. If we define  $D_u$  and  $D_d$  as the mass diagonal matrices of the up- and down-type quarks respectively, the transformations are

$$U_L^u M_u U_R^{u\dagger} = D_u, \quad U_L^d M_d U_R^{d\dagger} = D_d, \quad V_{CKM} = U_L^u U_L^{d\dagger}, \quad (53)$$

and the squared mass matrices  $H_u$  and  $H_d$  are

$$H_u = M_u M_u^\dagger, \quad H_d = M_d M_d^\dagger. \quad (54)$$

For simplicity, we assume that the quark mass matrices  $M_u$  and  $M_d$  are Hermitian. If we take a case in which  $M_d$  is very close to the diagonal matrix, or in other words  $U_L^d$  and  $U_R^d$  are very close to the unit matrix with very small off-diagonal terms, we have

$$V_{CKM} \sim U^u U^{d\dagger} \sim U^u, \quad (55)$$

where we have transformed away the right-handed effects and make them the same as the left-handed ones. Then the mass matrix of the up-type quarks turns out as

$$M_u \sim V_{CKM}^\dagger D_u V_{CKM}. \quad (56)$$

At the GUT scale, the CKM quark mixing matrix is given by [27]

$$V_{CKM} = \begin{pmatrix} 0.9754 & 0.2205 & -0.0026i \\ -0.2203e^{0.003^\circ i} & 0.9749 & 0.0318 \\ 0.0075e^{-19^\circ i} & -0.0311e^{1.0^\circ i} & 0.9995 \end{pmatrix}, \quad (57)$$

and  $D_u$  and  $D_d$  are

$$D_u = m_t \begin{pmatrix} 0.0000139 & 0 & 0 \\ 0 & 0.00404 & 0 \\ 0 & 0 & 1 \end{pmatrix}, \quad D_d = m_b \begin{pmatrix} 0.00141 & 0 & 0 \\ 0 & 0.0280 & 0 \\ 0 & 0 & 1 \end{pmatrix}, \quad (58)$$

so that the SM fermion mass matrices (we exclude the phases in this discussion) that we would like to match are given by

$$|M_u| = m_t \begin{pmatrix} 0.000266 & 0.00109 & 0.00747 \\ 0.00109 & 0.00481 & 0.0310 \\ 0.00747 & 0.0310 & 0.999 \end{pmatrix}, \quad |M_d| = D_d = m_b \begin{pmatrix} 0.00141 & 0 & 0 \\ 0 & 0.0280 & 0 \\ 0 & 0 & 1 \end{pmatrix}. \quad (59)$$

We use the relation  $\frac{m_\tau}{m_b} = 1.58$ , as well as require the eigenmasses of the leptons to be

$$\{m_e, m_\mu, m_\tau\} = m_\tau \{0.000217, 0.0458, 1\}. \quad (60)$$

## B. The Numerical Results

As mentioned above, there are six Higgs states in this model, and only three of them can provide the SM fermion Yukawa couplings from three-point functions on the second torus. And from Eq. (45) we can see explicitly only three linear combinations of the VEVs dominate the SM fermion mass matrices. To fit the diagonal terms in the up-type quark mass matrix, we have a limited number of degrees of freedom to work with on the off-diagonal mixings. Thus, it is hoped that the four-point corrections will improve this situation. In short, the situation for the Yukawa couplings of this model is not as ideal as the model analyzed in [17] due to the highly dependent relation between the diagonal and off-diagonal terms which results from fewer Higgs fields. Therefore, for the best fits to the SM fermion masses and mixings at the GUT scale, we will form the Yukawa mass matrices such that the diagonal terms result from both the three-point and four-point couplings, while the off-diagonal elements arise strictly from the four-point corrections. Since we also expect the down-type quark mass matrix to be diagonal, it is necessary to choose reasonably small off-diagonal terms for the mixing of the first two quark generations, so we set the Kähler parameter  $\frac{3J^{(2)}}{\alpha'} = 30.0$ .

### 1. Quantum Contributions

As mentioned above, the quantum contributions from the three-point and the four-point interactions can be ignored since they are able to be absorbed into the VEVs of the vector-like fields:

$$v'_i{}^\Phi = Z_{3q} v^\Phi ; \quad u'_i w'_j = Z_{4q} u_i w_j . \quad (61)$$

However it is interesting to study how much they may affect the VEVs. The angles between the branes on the second torus are

$$\lambda\pi = \angle ab = \angle bb' = \pi/2 ; \quad \nu\pi = \angle ac = \angle b'c = \pi/4 , \quad (62)$$

so from Eqs. (29) and (26) we have

$$Z_{3q}^{(2)} \sim 12.95 ; \quad Z_{4q}^{(2)}(x)|_{x \sim 0.5} \sim 120.8 . \quad (63)$$

In this case, the plot of  $Z_{4q}$  as a function of  $x$  in the range  $x = (0, 1)$  is shown in Figure 4, where we see that  $Z_{4q}$  approaches its three-point function limits of the corresponding fields when  $x$  approaches 0 or 1 as a constant, so we confine our interest of  $Z_{4q}$  near  $x = 0.5$ . We find that  $Z_{4q}/Z_{3q} \sim \mathcal{O}(10)$ .

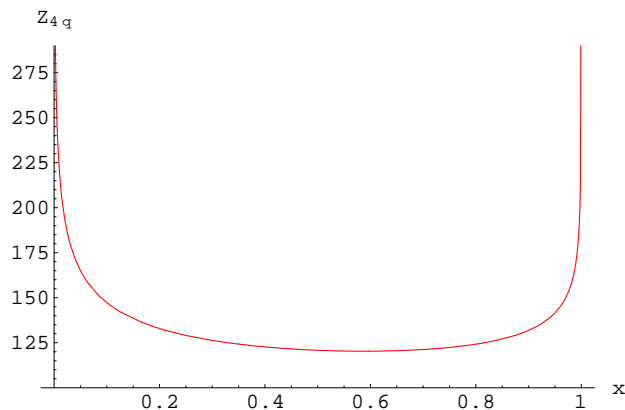


FIG. 4:  $Z_{4q}$  as a function of  $x$  in the range  $x = (0, 1)$ .

### 2. Yukawa Couplings from Three-Point Functions

Let us first consider the SM fermion Yukawa couplings only from the three-point functions. For the best fits, we set appropriate values of  $A_3^\Phi v^\Phi + D_3^\Phi v^\Phi$  to exactly match the diagonal terms of

$\Phi \backslash$ Parameters	$\epsilon^{(2)}$ (shift)	$A^\Phi$	$B^\Phi$	$C^\Phi$	$A_3^\Phi$	$D_3^\Phi$	$A_3^\Phi v_1^\Phi + D_3^\Phi v_4^\Phi$	$A_3^\Phi v_2^\Phi + D_3^\Phi v_5^\Phi$	$A_3^\Phi v_3^\Phi + D_3^\Phi v_6^\Phi$
$\Phi = u$ up quarks	0	1	0.000028	0.000028	1	0	$0.000266m_t$	$0.00481m_t$	$1.0m_t$
$\Phi = d$ down quarks	0.0775	0.567749	0	0.002094	1	0	$0.00248m_b$	$0.0493m_b$	$1.761m_b$
$\Phi = l$ leptons	0	1	0.000028	0.000028	0.901	$\sim 0$	$0.00224m_b$	$0.0444m_b$	$1.587m_b$

TABLE V: The matrix elements and the parameters when only trilinear Yukawa couplings considered. Note that  $v_i^d = v_i^l$ .

the SM fermion mass matrices at the GUT scale in Eqs. (59) and (60). The parameters and the VEVs in the quark and lepton mass matrices are listed in Table V.

The SM fermion mass matrices from the three-point function contributions are

$$\begin{aligned}
|M_{3u}| \sim m_t & \begin{pmatrix} 0.000266 & 0.000028 & 1.34 \cdot 10^{-7} \\ 0.000028 & 0.00481 & \sim 0 \\ 1.34 \cdot 10^{-7} & \sim 0 & 1.0 \end{pmatrix}, \quad |M_{3d}| \sim m_b \begin{pmatrix} 0.00141 & 0.00369 & 0 \\ 0 & 0.0280 & 5.19 \cdot 10^{-6} \\ 0.000103 & 0 & 1.0 \end{pmatrix}, \\
|M_{3l}| \sim m_b & \begin{pmatrix} 0.00224 & 0.0000444 & 1.24 \cdot 10^{-6} \\ 0.0000444 & 0.0444 & \sim 0 \\ 1.24 \cdot 10^{-6} & \sim 0 & 1.568 \end{pmatrix}. \quad (64)
\end{aligned}$$

Therefore, with only three-point functions, we can obtain the correct SM quark masses, and tau lepton mass. However, the quark CKM mixings are too small, and the electron and muon masses are far from the desired values.

### 3. Yukawa Couplings from Three-Point and Four-Point Functions

Let us study the SM fermion masses and mixings from both three-point and four-point functions. To be concrete, we present the SM fermion mass matrices from three-point and four-point functions separately in our best fits. First, we present the parameters and the VEVs for three quark and lepton mass matrices of the Yukawa couplings from the three-point functions in Table VI.

$\Phi \backslash$ Parameters	$\epsilon^{(2)}$ (shift)	$A^\Phi$	$B^\Phi$	$C^\Phi$	$A_3^\Phi$	$D_3^\Phi$	$A_3^\Phi v_1^\Phi + D_3^\Phi v_4^\Phi$	$A_3^\Phi v_2^\Phi + D_3^\Phi v_5^\Phi$	$A_3^\Phi v_3^\Phi + D_3^\Phi v_6^\Phi$
$\Phi = u$ up quarks	0	1	0.000028	0.000028	1	0	$0.0000250m_t$	$0.000262m_t$	$0.981m_t$
$\Phi = d$ down quarks	0.0775	0.567749	0	0.002094	1	0	$0.002820m_b$	$0.08784m_b$	$1.754m_b$
$\Phi = l$ leptons	0	1	0.000028	0.000028	0.901	$\sim 0$	$0.002541m_b$	$0.07916m_b$	$1.581m_b$

TABLE VI: The matrix elements in terms of parameters. Note  $v_i^d = v_i^l$ .

The SM fermion mass matrices from the three-point interactions are

$$\begin{aligned}
|M_{3u}^{3pt}| &\sim m_t \begin{pmatrix} 0.0000250 & 0.0000275 & \sim 0 \\ 0.0000275 & 0.000262 & \sim 0 \\ \sim 0 & \sim 0 & 0.981 \end{pmatrix}, \quad |M_{3d}^{3pt}| \sim m_b \begin{pmatrix} 0.00160 & 0.00367 & 0 \\ 0 & 0.0499 & 0.00000591 \\ 0.000184 & 0 & 0.996 \end{pmatrix}, \\
|M_{3l}^{3pt}| &\sim m_b \begin{pmatrix} 0.00254 & 0.0000443 & 2.22 \cdot 10^{-6} \\ 0.0000443 & 0.0792 & 7.12 \cdot 10^{-8} \\ 2.22 \cdot 10^{-6} & 7.12 \cdot 10^{-8} & 1.581 \end{pmatrix}. \tag{65}
\end{aligned}$$

Second, for the Yukawa couplings from the four-point functions, we present the parameters and the shifts of the D-branes in Table VII, and the VEVs of three  $S_L^i$  and  $H_{u,d}^i$  in Table VIII.

$\Phi \backslash$ Parameters	$\epsilon^{(2)}$	$\epsilon_b^{(2)}$	$\mathcal{A}^\Phi$	$\mathcal{B}^\Phi$	$\mathcal{C}^\Phi$	$\mathcal{D}^\Phi$	$\mathcal{E}^\Phi$	$\mathcal{F}^\Phi$	$\mathcal{G}^\Phi$	$\mathcal{H}^\Phi$	$\mathcal{I}^\Phi$
$\Phi = u$ up quarks	0	0.32	0.000064	0.679089	0.679089	0.000012	0.670140	0.670140	1.335992	0.000029	0.000029
$\Phi = d$ down quarks	0.08	0.03	0.595678	0	0.00257000	0.000007	0.028872	0.001674	0.000313	0.000595	0.073686
$\Phi = l$ leptons	0	0.03	0.932776	0.000031	0.000031	0.000004	0.165161	0.165161	0.000171	0.187111	0.187111

TABLE VII: The matrix elements in terms of parameters.

$\Phi \backslash$ Parameters	$u_1(M_s)$	$u_2(M_s)$	$u_3(M_s)$	$w_1(m_b)$	$w_2(m_b)$	$w_3(m_b)$
$\Phi = u$ up quarks	0.08	0.06	0.23	0.0148	0.18	0.003
$\Phi = d$ down quarks	0.08	0.06	0.23	-0.004	-0.612	0.03
$\Phi = l$ leptons	0.08	0.06	0.23	-0.004	-0.612	0.03

TABLE VIII: The VEVs of three  $S_L^i$  and  $H_{u,d}^i$ .

The SM fermion mass matrices from the four-point interactions are

$$\begin{aligned}
|M_{4u}^{4pt}| &\sim m_t \begin{pmatrix} 0.000241 & 0.00106 & 0.00750 \\ 0.00106 & 0.00455 & 0.0285 \\ 0.00750 & 0.0285 & 0.0192 \end{pmatrix}, \quad |M_{4d}^{4pt}| \sim m_b \begin{pmatrix} -0.000191 & -0.00359 & 0.0000688 \\ -0.0000361 & -0.0219 & 0.000104 \\ 0.000158 & -0.00406 & 0.00409 \end{pmatrix}, \\
|M_{4l}^{4pt}| &\sim m_b \begin{pmatrix} -0.000299 & -0.00920 & 0.000223 \\ -0.00920 & -0.0343 & -0.0229 \\ 0.00657 & -0.0229 & 0.00623 \end{pmatrix}. \tag{66}
\end{aligned}$$

Therefore, we sum over the two contributions, and obtain

$$\begin{aligned}
 |M_u| &\sim m_t \begin{pmatrix} 0.000266 & 0.00109 & 0.00750 \\ 0.00109 & 0.00481 & 0.0285 \\ 0.00750 & 0.0285 & 1.0 \end{pmatrix}, \quad |M_d| \sim m_b \begin{pmatrix} 0.00141 & 0.0000828 & 0.0000688 \\ -0.0000361 & 0.028 & -0.0000979 \\ 0.0000258 & -0.00406 & 1.0 \end{pmatrix}, \\
 |M_l| &\sim m_b \begin{pmatrix} 0.00224 & -0.00915 & 0.000223 \\ -0.00915 & -0.0449 & -0.0229 \\ 0.000223 & -0.0229 & 1.587 \end{pmatrix}, \quad (67)
 \end{aligned}$$

and the mass eigenvalues of the leptons are

$$\{m_e, m_\mu, m_\tau\} = m_b\{0.000348, 0.0464, 1.588\} = m_\tau\{0.000219, 0.0292, 1\}. \quad (68)$$

Comparing with the SM fermion masses and mixings in Eqs. (59) and (60), we find that the off-diagonal terms of the up-type quark mass matrix are basically from the four-point contributions, and it is quite difficult to fit exactly the same off-diagonal terms due to the four-point function matrix structure. For the down-type quark matrix, we still cannot eliminate the off-diagonal terms. However, we can suppress them such that they are in an acceptable range. In addition, the quark CKM mixing matrix is

$$V_{CKM} \simeq \begin{pmatrix} 0.977 & 0.212 & 0.00109 \\ 0.212 & 0.977 & 0.0298 \\ 0.00738 & 0.0289 & 0.9996 \end{pmatrix}, \quad (69)$$

and then there are some deviations for the quark mixing terms in Eq. (57), but they are in an acceptable range. Finally, we are able to decrease the electron mass eigenvalue to the correct value by the off-diagonal terms from the four-point contributions, but the muon mass eigenvalue is still about 36% smaller than the desired value.

## V. CONCLUSION

We have discussed corrections to the SM fermion Yukawa couplings in intersecting D6-brane models due to four-point interactions and presented a working example, and demonstrated that these corrections can improve the best fits for the SM fermion masses and mixings. In a concrete model, we first calculated the SM fermion masses and mixings from three-point functions. Considering only these contributions, we can obtain the correct quark masses and tau lepton mass, but the CKM quark mixings are not large enough, and the electron and muon masses are far from the

desired values. After including the corrections to the SM fermion Yukawa couplings from four-point functions, we can obtain the correct quark masses and CKM mixings, and the correct electron and tau lepton mass scales. However, the muon mass is still around 36% smaller than the desired value.

In this work, we have not considered the moduli stabilization problem, and have essentially treated the moduli VEVs as free parameters. As is obvious, there exists fine-tuning in our discussion of the D-brane positions and the Higgs VEVs. The four-point interactions have nine dependent worldsheet instanton parameters as well as six additional string-scale Higgs particles and their VEVs. To stabilize these undetermined variables, one may consider a  $\mathbb{Z}_2 \times \mathbb{Z}'_2$  orientifold model with discrete torsion where the D-branes wrap rigid cycles, thus stabilizing the open-string moduli. In this case, one would also expect corrections to the Yukawa couplings from D-brane instantons. Indeed, E2-branes required for this construction must also wrap rigid cycles, so there is additional motivation to consider this background. We plan to pursue these possibilities in our future research.

### Acknowledgements

This research was supported in part by the Mitchell-Heep Chair in High Energy Physics (CMC), by the Cambridge-Mitchell Collaboration in Theoretical Cosmology (TL), and by the DOE grant DE-FG03-95-Er-40917 (DVN).

- 
- [1] M. Berkooz, M. R. Douglas and R. G. Leigh, Nucl. Phys. B **480**, 265 (1996) [arXiv:hep-th/9606139].
  - [2] C. Bachas, [arXiv:hep-th/9503030].
  - [3] R. Blumenhagen, M. Cvetič, P. Langacker and G. Shiu, Ann. Rev. Nucl. Part. Sci. **55**, 71 (2005) [arXiv:hep-th/0502005].
  - [4] R. Blumenhagen, B. Kors, D. Lust and S. Stieberger, Phys. Rept. **445**, 1 (2007) [arXiv:hep-th/0610327].
  - [5] G. Aldazabal, S. Franco, L. E. Ibanez, R. Rabadan and A. M. Uranga, JHEP **0102**, 047 (2001) [arXiv:hep-ph/0011132].
  - [6] L. E. Ibanez and A. M. Uranga, [arXiv:hep-th/0609213].
  - [7] R. Blumenhagen, M. Cvetič and T. Weigand, [arXiv:hep-th/0609191].
  - [8] B. Florea, S. Kachru, J. McGreevy and N. Saulina, JHEP **0705**, 024 (2007) [arXiv:hep-th/0610003].
  - [9] S. A. Abel and M. D. Goodsell, JHEP **0710**, 034 (2007) [arXiv:hep-th/0612110].
  - [10] M. Billo, M. Frau, I. Pesando, P. Di Vecchia, A. Lerda and R. Marotta, JHEP **0712**, 051 (2007) [arXiv:0709.0245 [hep-th]].
  - [11] D. Cremades, L. E. Ibanez and F. Marchesano, JHEP **0307**, 038 (2003) [arXiv:hep-th/0302105].
  - [12] N. Chamoun, S. Khalil and E. Lashin, Phys. Rev. D **69**, 095011 (2004) [arXiv:hep-ph/0309169].

- [13] N. Kitazawa, T. Kobayashi, N. Maru and N. Okada, *Eur. Phys. J. C* **40**, 579 (2005) [arXiv:hep-th/0406115].
- [14] B. Dutta and Y. Mimura, *Phys. Lett. B* **633**, 761 (2006) [arXiv:hep-ph/0512171]; *Phys. Lett. B* **638**, 239 (2006) [arXiv:hep-ph/0604126].
- [15] M. Cvetič, T. Li and T. Liu, *Nucl. Phys. B* **698**, 163 (2004) [arXiv:hep-th/0403061].
- [16] C.-M. Chen, T. Li and D. V. Nanopoulos, *Nucl. Phys. B* **740**, 79 (2006) [arXiv:hep-th/0601064].
- [17] C.-M. Chen, T. Li, V. E. Mayes and D. V. Nanopoulos, [arXiv:hep-th/0703280]; *Phys. Rev. D* **77**, 125023 (2008) arXiv:0711.0396 [hep-ph].
- [18] J. R. Ellis and M. K. Gaillard, *Phys. Lett. B* **88**, 315 (1979); D. V. Nanopoulos and M. Srednicki, *Phys. Lett. B* **124**, 37 (1983).
- [19] S. Kalara, J. L. Lopez and D. V. Nanopoulos, *Phys. Lett. B* **245**, 421 (1990); *Nucl. Phys. B* **353**, 650 (1991).
- [20] D. Lust, P. Mayr, R. Richter and S. Stieberger, *Nucl. Phys. B* **696**, 205 (2004) [arXiv:hep-th/0404134].
- [21] M. Bertolini, M. Billo, A. Lerda, J. F. Morales and R. Russo, *Nucl. Phys. B* **743**, 1 (2006) [arXiv:hep-th/0512067].
- [22] M. Cvetič and I. Papadimitriou, *Phys. Rev. D* **68**, 046001 (2003) [Erratum-ibid. *D* **70**, 029903 (2004)] [arXiv:hep-th/0303083]; S. A. Abel and A. W. Owen, *Nucl. Phys. B* **663**, 197 (2003) [arXiv:hep-th/0303124].
- [23] S. A. Abel and A. W. Owen, *Nucl. Phys. B* **682**, 183 (2004) [arXiv:hep-th/0310257].
- [24] S. Hamidi and C. Vafa, *Nucl. Phys. B* **279**, 465 (1987).
- [25] L. J. Dixon, D. Friedan, E. J. Martinec and S. H. Shenker, *Nucl. Phys. B* **282**, 13 (1987); J. J. Atick, L. J. Dixon, P. A. Griffin and D. Nemeschansky, *Nucl. Phys. B* **298**, 1 (1988).
- [26] T. T. Burwick, R. K. Kaiser and H. F. Muller, *Nucl. Phys. B* **355**, 689 (1991).
- [27] H. Fusaoka and Y. Koide, *Phys. Rev. D* **57**, 3986 (1998) [arXiv:hep-ph/9712201]; G. Ross and M. Serna, arXiv:0704.1248 [hep-ph].